ANALYSIS AND PREDICTION OF SPATIO-TEMPORAL FLAME DYNAMICS

Mauro Annunziato[1] *, Stefano Pizzuti*[1] *and Lev S. Tsimring*[2]

[1] ENEA – Casaccia Research Centre
Via Anguillarese 301, 00060 S.M.di Galeria (Rome), Italy
{mauro.annunziato,stefano.pizzuti}@casaccia.enea.it

[2] Institute for Nonlinear Science, University of California,San Diego
La Jolla, CA 92093-0402, U.S.A.
ltsimring@ucsd.edu

Abstract - *In this paper we discuss novel methods of classification and prediction of spatio-temporal dynamics in extended systems. We tested these methods on simulated data for the Kuramoto-Sivashinsky equation that describes unstable flame front propagation in uniform mixtures.*

I. INTRODUCTION

Accurate measurement and control of critical parameters is a vital issue in operation of combustion cameras used in waste incinerators. Instrument calibration, periodic surveillance tests, plant performance monitoring, and forced outages are costly activities. From a fundamental perspective, combustion represents a very important example of complex spatio-temporal dynamics in extended systems. Flame front is typically unstable giving rise to irregular fluctuations.

Our ability to analyze temporal chaos from physical observations taken at a fixed spatial point has reached a quite well developed stage [1,2,3]. One can take a scalar data stream $a(n) = a(t_0+n\tau)$ observed at intervals τ, and reconstruct a vector state space [4,5] from a(n) and its time lags a(n+kT), where T is a multiple of τ chosen by considerations of average mutual information [6] in the data. The dimension of the vector space is chosen using the method of false nearest neighbors [2,3,7] which is accurate even for small data sets and quite robust in the presence of noise.

Much less developed is our ability to analyze data from spatio-temporal systems where the dynamical degrees of freedom are fields z(x,t). The main goal of this study is to develop methods for the extraction from observed data in space and time (i) of information on the size and features of the dynamical phase space (analogous to phase space reconstruction in temporal chaos), and (ii) of information on how to classify spatio-temporal dynamics. With this we develop methods to build low dimensional models which have predictive power for applications in monitoring and to controlling plant operation. In this work, we introduce the algorithms for analysis of the spatio-temporal data and apply them to simulated combustion data generated by the Kuramoto-Sivashinsky equation [8]. This equation describes the propagation of unstable flame front in uniform combustible mixtures.

II. KURAMOTO-SIVASHINSKY EQUATION

As an example we consider here spatio-temporal data obtained by numerical integration of the Kuramoto-Sivashinsky equation

$$u_t + u_x^2 + \sigma u_{xx} + u_{xxxx} = 0 \qquad (1)$$

at values of σ which correspond to the regime of extensive spatio-temporal chaos. This well-known equation describes unstable regimes of flame front propagation [8]. For $\sigma>0$ the uniform flame front u=0 is unstable with respect to long-wave periodic perturbations $\propto \sin kx$. The most unstable wavenumber is $k_0=\sigma^{1/2}$. Nonlinearity leads to saturation of the instability and the onset of persistent non-stationary spatially non-uniform regime (cellular flame). The spatial and temporal scales of the fluctuations decrease with the increase of the control parameter σ.

To generate simulated flame front position data, we employed the numerical integration scheme which used split-step pseudo-spectral method with 1024 mesh points, time step 0.1 and space step 0.1 (system size L=30.5). Figure 2,b shows sample space-time plot u(x,t) for Eq.(1) for $\sigma=0.5$ and $\sigma=3.0$ starting from small-amplitude random initial conditions for $0<t<200$.

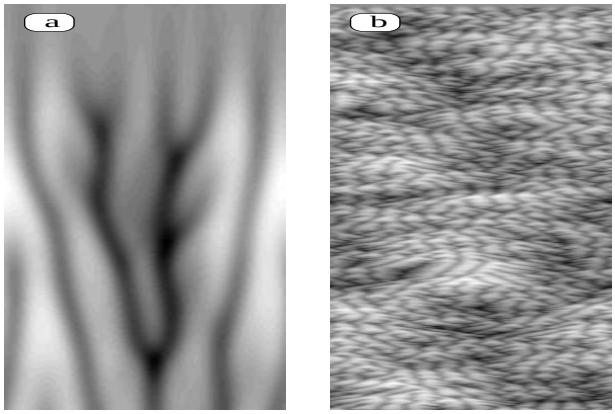

Figure 1. Spatio-temporal evolution of the flame front within the Kuramoto-Sivashinsky equation (1): *a* slow long-wave perturbations at σ=0.5; *b* highly-chaotic regime at σ=3.0 (0<x<30.5, 0<t<200).

III. PREDICTION

Now we proceed to the analysis of the spatio-temporal data for the Kuramoto-Sivashinsky equation in the chaotic regime at σ=3.0. Figure 3 shows the mutual information I(X,T) as a function of spatial delay X and temporal delay T. The first minimum of mutual information occurs at X=10 and T=21 (measured in units of sample times).

The next step is to determine the optimal structure of the embedding vector. We calculated prediction error for various templates (Fig.2), using local linear prediction 1 time lag ahead for Kuramoto-Sivashinsky data.

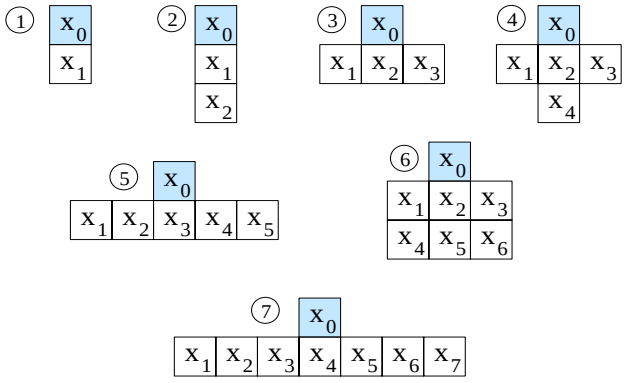

Figure 2. Templates for embedding spatio-temporal data in 1..7 dimensions. x_0 denotes the value to be predicted.

We used time lag 0.2 and local linear maps. Table 1 reports the prediction error as a function of the spatial lag for different templates (figure 2)

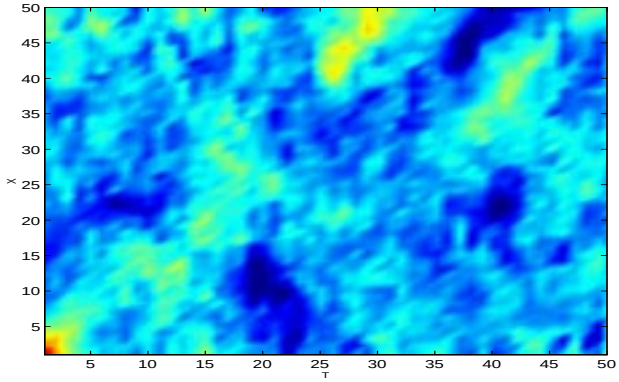

Figure 3. Mutual information as a function of space and time delays for Kuramoto-Sivashinsky equation (1) with σ=3.

	Templates						
Space lag	1	2	3	4	5	6	7
1	0.23181	0.13799	0.18483	0.13423	0.17005	0.12127	0.15650
3	0.23181	0.137838	0.15389	0.12960	0.12995	0.11182	0.11226
5	0.23181	0.137807	0.14323	0.12608	0.10476	0.11278	0.09320
7	0.23181	0.137853	0.13342	0.12198	0.09598	0.10953	0.08950
9	0.23181	0.137839	0.12504	0.11850	0.09217	0.11925	0.09318
11	0.23181	0.137814	0.12139	0.11961	0.09300	0.1229	0.10821
13	0.23181	0.137779	0.12674	0.11673	0.10587	0.12680	0.13272

Tab. 1: prediction error as a function of the spatial lag for different templates

As can be seen from the table, the minimal prediction errors occur for the Template 5 and space lag 9. Similar calculations can be made for other systems of interest.

Now we turn to the system monitoring using prediction errors as a measure of system changes. We integrated the Kuramoto-Sivashinsky equation (1) with σ=3.5 from t=0 to 10. Then we changed the value of σ to 3.0 and run the system until t=60. We used the last portion of the data 40.0<t<60.0 for building the predictive model, and used it for prediction. Figure 4 presents the results of this numerical experiment. In Figure 4,a we show the waveform a(x,t), and in Figure 4,b the prediction error normalized by the standard deviation is shown. The prediction error is large in the first part of the

data where the data does not correspond to the model, and it decreases rapidly in the domain where parameters of the model and data correspond to each other.

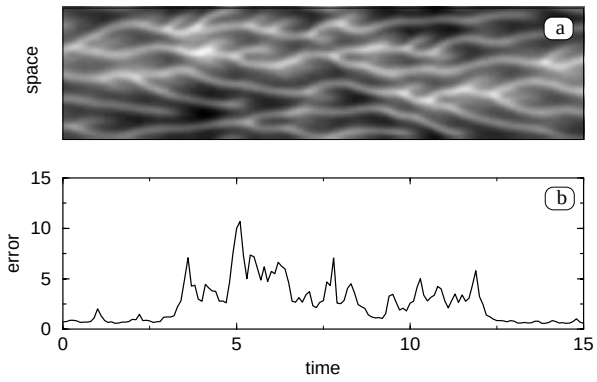

Figure 4. Waveform (a) and space-averaged prediction error as a function of time (b) for Kuramoto-Sivashinsky equation (8) with varying σ: σ=3.0 for 0<t<3 and 12<t<15; σ=3.5 for 3<t<12.

IV. RECOGNITION OF CHAOTIC REGIMES

When we are dealing with a chaotic process one of the most important tasks is that of system classification, namely the recognition of the current chaotic regime, and to achieve this goal we need suitable discriminants and proper criteria to select them.

In this context we carried out two supervised strategies able to select the best among 27 parameters, the dynamic moments, in order to identify two given chaotic regimes of the Kuramoto-Sivashinsky (1) flame model corresponding to two different values of parameter σ (σ=2.7, σ=3).

In the following paragraphs we shall describe the dynamic moments methodology and the strategies we developed to select them.

A. Dynamic Moments

In 1996, Annunziato and Abarbanel elaborated a new methodology for classification problems based on the attractor description using few discriminant parameters (*Dynamic Moments*). This methodology has been successfully applied to the identification of the multiphase flow regime in oil production plants using differential pressure sensors [13], to the characterisation of combustion chambers for gas turbines using acoustical sensors and sensors for local thermal release, to the characterisation of combustibles pollutants in conventional chambers using CCD camera [14], and finally to the identification of working state of waste incinerators using still CCD camera.

The basic idea is to compute a series of "moments of inertia" for the attractor fir different orders and dimensions. We build a series of shape descriptors, named *dynamic moments*. The technique consists of specifying certain points or axes or planes with respect to which the distances to every point of the attractor are computed.

Generally, the dimension of the space in which we compute the dynamic moments should be equal to the number of the dimensions of the chaotic process. However, if the chaotic process has high dimension, for classification purposes it is possible to extract discriminant characteristics by computing the dynamics moments in a lower dimension space, provided that the classes are well enough separated. Obviously, for dimensions 2 and 3 we have easily visualizable geometric interpretation, while for higher dimensions we lose visual representation and reduce the procedure to an algorithmic selection.

As example here we describe the 2D dynamic moments.

When we work in two dimensions we are projecting the attractor on the plane, so we consider only two components of the signal: $x_i=s(it)$ and $y_i=s(it+T)$ where t is the acquisition time and T is the time lag which we vary from 0 to a high value that makes the components totally independent. We compute the distances between every point on the attractor and two axes, the bisector of first-third quadrant (called *principal axis*) and second-fourth quadrant, and the origin:

$$d_{1,i} = \frac{\sqrt{2}}{2}(x_i - y_i) \tag{2}$$

$$d_{2,i} = \frac{\sqrt{2}}{2}(x_i + y_i) \tag{3}$$

$$d_{3,i} = \sqrt{x_i^2 + y_i^2} \tag{4}$$

Using these distances we are able to define moments of order j:

$$M_{m,j}(T) = \frac{\sum_{i=1}^{N} {d_{m,i}}^j}{N} \tag{5}$$

where N is the number of samples and m=1,2,3 the distance considered.

For T=0, $x_i=y_i$, and the attractor is compressed on the principal axis; when T increases, these moments

describe the morphological evolution during the unfolding process of the attractor. The moments evolve from the linear value (for T=0) to nonlinear one. Finally we can outline that the even moments are always positive and describe the scatter of the attractor, while the odd moments are symmetry descriptors.
Although 2D moments can be accurate enough to characterize chaotic processes, sometimes it can be necessary to extend moment calculation to higher dimensions in order to have parameters more sensitive to the fine characteristics of the attractor. The reader interested in detail in this topic can refer to [13].

B. Selection Strategies

Now we describe the two strategies we used to select the most significant among 27 different dynamic moments. Such moments differ for order, dimension and distance computation.
Both strategies we are about to outline are supervised, in the sense that they use an a priori given parameter describing the chaotic regime and they differ by the cost function applied.

C. Classes Overlapping

The first criterion is based on the principle of minimising the overlapping among the distribution of the data of different classes in the space of the selected discriminants. The idea is that *n* moments are good if they provide a good separability among the classes to be recognised.
To perform this task we defined the following cost function on two classes:

$$f(m_1,...,m_n) = 1 - \frac{\sum_{1=1}^{k} C_1(i)C_2(i)}{\sqrt{\sum_{i=1}^{k} C_1^2(i) \sum_{i=1}^{k} C_2^2(i)}}, \qquad (6)$$

where *n* is the number of moments to be selected, *k* is the number of cells in which the n-dimensional space has been partitioned, $C_j(i)$ is the density of class j in cell i.

D. Mutual Information

The second approach is based on the idea that if discriminants are independent from classification, then those discriminants will be not suitable for that classification. In this way as cost function we used the mutual information between classification and moments.
To select the best moment we search for the maximum of the mutual information

$$I(m_i,c) = H(m_i)+H(c)–H(m_i,c), \qquad (7)$$

where

$$H(m_i) = -\Sigma P(m_i)\log_2(P(m_i)) \qquad (8)$$

is the entropy of the distribution of the i-th moment, H(c) is the entropy of the classification distribution, and

$$H(m_i,c) = -\Sigma P(m_i , c)\log_2(P(m_i , c)) \qquad (9)$$

is the joint entropy between the i-th moment and the classification. Note that if the distributions of the i-th moment and the classification are statistically independent, than the mutual information $I(m_i,c)$ turns into zero.
Furthermore, to select the best pair of moments we use the following formula for the mutual information between a pair of moments and classification,

$$I(m_i,m_j,c) = H(m_i)+H(m_j)+H(c)–H(m_i,m_j,c) \qquad (10)$$

where $H(m_i)$ is the entropy of the distribution of the i-th moment, H(c) is the entropy of the classification distribution and $H(m_i,m_j,c)$ is the joint entropy among moment i, moment j and classification.

E. Results

We tested the approaches previously outlined on two known different chaotic regimes the Kuramoto-Sivashinsky (1) equation generating 900 points for each of them. To stress the statistical instability of the moments and the overlapping between the classes we considered each point on a short time (1000 steps).
In the following tables we report the rankings given by the two approaches on one and two discriminants.

Overlapping		Mutual Information	
10	0.9623	10	0.781512
1	0.962176	1	0.779873
4	0.947696	4	0.735537
13	0.927983	13	0.677474
16	0.919490	16	0.666863

Tab.2 : comparison of the best 5 single moments

Overlapping		Mutual Information	
10,20	0.977774	8,10	0.834606
1,8	0.977741	1,8	0.833297
1,20	0.977467	10,20	0.830875
8,10	0.977445	1,20	0.829037
1,23	0.977366	10,23	0.824313

Tab.3 : comparison of the best 5 couples of moments

From these results we conclude the similarity between the two approaches.
In figure 5 we report as an example the distribution of the two "good" moments for the two different regimes studied here.

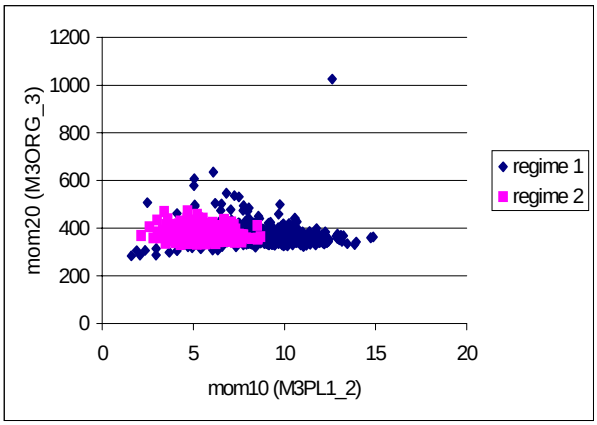

Figure 5. Distribution of the data in the moments space

Finally to validate the results we computed the classification rate using good and bad moments. To perform this task we used a simple multilayer neural network with input the values of two selected moments. From this experimentations we got a rate of about 95% succesful classification using the good ranked moments and a rate of about 60% for the bad ones.
This result is remarkable because it tells us that with only two parameters we may be able to identify the dinamical state of the flame.

V. Conclusions

In this paper we discussed novel methods of analysis of spatio-temporal dynamics in extended systems. In particular we tested the proposed methods for prediction and and recognition on simulated data for the Kuramoto-Sivashinsky equation that describes the unstable flame front propagation in uniform mixtures. The positive results obtained in numerical studies, let us hope that the developed tools can also be applied to real experimental data from the combustion cameras and incinerators.

References

[1] J.-P.Eckmann and D. Ruelle, Ergodic Theory of Chaos and Strange Attractors, *Rev. Mod. Phys.*, **57**, 617-656 (1985).

[2] H.D.I.Abarbanel, R.Brown, J.J.Sidorowich, and L.S.Tsimring. The analysis of observed chaotic data in physical systems, *Rev. Mod. Phys.*, **64**, no.5, 1331-1393 (1993).

[3] H.D.I.Abarbanel, *Analysis of Observed Chaotic Data*, Springer, New York (1996).

[4] R.Mane, in *Dynamical Systems and Turbulence*, Warwick 1980, Lecture Notes in Mathematics, **898**, ed. D.Rand and L.S.Young (Springer, Berlin.1981).

[5] F.Takens, in *Dynamical Systems and Turbulence*, Warwick 1980, Lecture Notes in Mathematics, **898**, ed. D.Rand and L.S.Young (Springer, Berlin, 1981).

[6] A.M.Fraser and H.L.Swinney, *Phys.Rev. A*, **33**, 1134 (1986); A.M.Fraser, Information and Entropy in Strange Attractors, *IEEE Trans. On Info. Theory*, *35*, 245 (1989); A.M.Fraser, *Physica D*, **34**, 391 (1989).

[7] M.B.Kennel, R.Brown, and H.D.I.Abarbanel, Determining Minimum Embedding Dimension using a Geometrical Construction, *Phys. Rev. A*, **45**, 3403-3411 (1992).

[8] G.I.Sivashinsky, Nonlinear Analysis of Hydrodynamic Instability in Laminar Flames, *Acta Astronomica*, **4**, 1177 (1977).

[9] L.S.Tsimring. Nested strange attractors in spatiotemporal chaotic systems, *Phys. Rev. E*, **48**, n.5, 3421 (1993).

[10] A.Torcini., A.Politi, G.P.Puccioni and C.D'Alessandro, Fractal Dimension of Spatially Extended Systems, *Physica D*, **53**, 85 (1991).

[11] L.N.Korzinov and M.I.Rabinovich, in *Applied Nonlinear Dynamics* (Saratov University Press), **2**, 59 (1994).

[12] A.Politi and A.Witt, Fractal dimension of Space-Time Chaos, *Phys. Rev. Lett.*, **82**, 3034 (1999).

[13] M.Annunziato, H.D.I.Abarbanel: "Non Linear Dynamics for Classification of Multiphase Flow Regimes", Int. Conf. Soft Computing, SOCO, Genova, 1999.

[14] M.Annunziato, I.Bertini, M.Piacentini, A.Pannicelli. *"Flame dynamics characterization by chaotic analysis of image sequences"*. 36 Int. HTMF Institute, Sacramento, CA, June 99.